

- no fluorescence as described (5) with anti-Fn and fluorescein isothiocyanate (FITC)-conjugated goat antibody to rabbit IgG. Similarly, immunofluorescence studies with antibodies specific for Fn, collagens I and III, vitronectin, laminin, and osteopontin were also done. Epifluorescence was photographed with a Zeiss Axiophot microscope.
22. E. Ruoslahti, *Annu. Rev. Biochem.* **57**, 375 (1988); R. O. Hynes, *Fibronectins* (Springer-Verlag, New York, 1990); M. A. Chernousov, F. J. Fogarty, V. E. Koteliansky, D. F. Mosher, *J. Biol. Chem.* **266**, 10851 (1991); Q. Zhang, W. J. Chechovich, D. M. Peters, R. M. Albrecht, D. F. Mosher, *J. Cell Biol.* **127**, 1447 (1994); C. Wu, V. M. Keivens, T. E. O'Toole, J. A. McDonald, M. H. Ginsberg, *Cell* **83**, 715 (1995); Q. Zhang and D. F. Mosher, *J. Biol. Chem.* **271**, 33284 (1996).
 23. W. A. Border and E. Ruoslahti, *J. Clin. Invest.* **90**, 1 (1992).
 24. Age-, sex-, and weight-matched UG^{+/+} (*n* = 3) and UG^{-/-} mice (*n* = 3) were killed and serum PLA₂ activities of each sample were measured in triplicate with a PLA₂-assay kit (Caymen Chemical) according to the instructions of the manufacturer. Protein concentrations in the sera were determined by Bradford assay (Bio-Rad), and specific activities of PLA₂ were determined.
 25. Using 24-well plates coated with human Fn (hFn) (Collaborative Biomedical Products), we incubated 3 μ l of ¹²⁵I-Fn (specific activity of 6 μ Ci/ μ g; ICN Biomedicals) in the absence and presence of either UG or Fn (10^{-12} to 10^{-6} M) in 500 μ l of Hanks' balanced salt solution (HBSS) at room temperature for 2 hours. SDS-PAGE and protein immunoblotting of all Fn with anti-UG failed to detect any UG contamination. The radiolabeled complex was washed twice with phosphate-buffered saline (PBS), solubilized in 1 N NaOH, and neutralized with 1 N HCl, and radioactivity was measured by a gamma counter. In a separate experiment ¹²⁵I-hFn (3 μ l) was incubated with 20 μ l (1 μ g/ μ l) of mouse Fn in 40 μ l of HBSS, pH 7.6, in the absence or presence of increasing concentrations of reduced UG (5 to 500 μ g) at room temperature for 2 hours. The samples were cross-linked with 0.20 mM DSS at room temperature for 20 min, boiled in SDS sample buffer for 5 min, electrophoresed on a 4 to 20% gradient SDS-polyacrylamide gel, and autoradiographed. In another experiment, 15 μ l of either denatured or nondenatured ¹²⁵I-collagen I (specific activity of 65.4 μ Ci/ μ g) was incubated with Fn in presence of reduced UG (250 μ g), affinity cross-linked, electrophoresed, and autoradiographed.
 26. Human Fn (500 μ g/150 μ l of PBS) was administered in the tail vein (27) of 2-month-old, ~22-g, UG^{+/+} and apparently healthy UG^{-/-} mice. Similarly, the control mice were injected with a mixture of 500 μ g of hFn either with equimolar concentrations of UG or BSA in 150 μ l of PBS. Twenty-four hours after the last injection, the mice were killed and various organs fixed in buffered formalin. Accumulation of hFn immunoreactivity in tissues was analyzed by immunofluorescence (6) with a monoclonal antibody to hFn (Gibco-BRL; clone 1) and FITC-conjugated rabbit antibody to mouse IgG (Cappel). In a separate experiment, UG^{+/+} mice were injected with 1 mg of Fn alone in 150 μ l of PBS daily for three consecutive days.
 27. E. Oh, M. Pierschbacher, E. Ruoslahti, *Proc. Natl. Acad. Sci. U.S.A.* **78**, 3218 (1981).
 28. Z. Zhang *et al.*, unpublished results.
 29. Fn matrix assembly and fibrillogenesis in cultured cells (CRL6336, American Type Culture Collection) were determined as described [D. F. Mosher, J. Sotile, C. Wu, J. A. McDonald, *Curr. Biol.* **4**, 810 (1992)].
 30. G. Mazzucco, E. Maran, C. Rollino, G. Monga, *Hum. Pathol.* **23**, 63 (1992); E. H. Strom *et al.*, *Kidney Int.* **48**, 163 (1995); K. J. M. Assmann, R. A. P. Koene, J. F. M. Wetzels, *Am. J. Kidney Dis.* **25**, 781 (1995); O. Gempferle, J. Neuweiler, F. Reutter, F. Hidebrandt, R. Krapf, *ibid.* **28**, 668 (1996).
 31. A Bam HI-Eco RI 3.2-kb DNA fragment containing exon-3 of 129/SVJ mouse UG gene (14) and its flanking sequences were subcloned into the corresponding site of the pPNW vector as described [K. Lei *et al.*, *Nature Genet.* **13**, 203 (1996)]. A 0.9-kb PCR-amplified fragment containing partial exon-2 and its flanking sequences with built-in Not I and Xho I sites were subcloned into the vector to generate the targeted construct pPNWUG. In pPNWUG, a 1.2-kb DNA fragment, including partial exon-2, was replaced with the PGK-*neo* cassette, disrupting the UG gene. Not I-linearized targeting construct DNA (25 μ g) was electroporated into ES R1 cells. Chimeric mice were mated with C57BL/6 strain of mice, and germline transmission of the mutated UG allele was identified by PCR and Southern blot analyses of offspring tail DNA. The genotyping of progeny was carried out by PCR with a set of *neo*-specific primers, *neo*-L (5'-ATA CGC TTG ATC CGG CTA CCT GCC-3') and *neo*-R (5'-CAT TTG CAC TGC CGG TAG AAC TCC-3'), which yield a 667-base pair (bp) DNA fragment. A 304-bp DNA fragment was generated with a set of UG-specific primers, mUG-L (5'-ACA TCA TGA AGC TCA CAG GTA TGC-3') and mUG-R (5'-GTG TGC ACG GTT CAA GCT TGT AGT-3'), derived from the region of the UG gene that was replaced by the PGK-*neo* cassette. After an initial denaturing step (95°C for 2 min), 40 cycles of PCR were performed (94°C for 1 min, 58°C for 1.5 min, 72°C for 1 min) with a final step at 72°C for 10 min, by using a Perkin-Elmer 480 DNA thermal cycler.
 32. The contributions of G.C.K. and C.-J.Y. in delineating the mechanism of UG action should be considered equal. We thank A. Nagy, R. Nagy, and W. Abramow-Newerly for ES R1 cells; L. Miele for statistical analyses; L. Miele and G. Mantile-Selvaggi for facilitating recombinant UG production in *Escherichia coli*; A. Kulkarni, K. M. Yamada, J. Chou, I. Owens, S. W. Levin, J. DeB. Butler, K.-J. Lei, and C.-J. Pan for their assistance, discussions, and suggestions, and Syntex Research for gancyclovir. Supported in part by a USPHS grant (number HL47620 to F.D.).

15 January 1997; accepted 27 March 1997

A Cellular Cofactor for the Constitutive Transport Element of Type D Retrovirus

Hengli Tang, Guido M. Gaietta, Wolfgang H. Fischer, Mark H. Ellisman, Flossie Wong-Staal*

A human nuclear protein that specifically interacts with the constitutive transport element (CTE) of simian retrovirus was identified as adenosine 5'-triphosphate-dependent RNA helicase A. This protein could bind to functional CTE but not to inactive CTE mutants. The interaction of helicase A with CTE was distinct from previously described helicase activity of this protein. Helicase A shuttled from the nucleus to the cytoplasm in the presence of a transcription inhibitor or in cells transiently overexpressing CTE-containing RNA. In vivo colocalization of helicase A and CTE was observed in experiments that combined in situ hybridization and immunostaining. These results suggest that helicase A plays a role in the nuclear export of CTE-containing RNA.

Normal cellular mRNAs are exported from the nucleus as fully spliced RNA. However, retroviruses need to export partially spliced or unspliced RNA to the cytoplasm, both as templates for protein synthesis and as genomic RNA to be packaged in progeny virions. The complex retroviruses, including the human pathogenic retroviruses human T cell leukemia virus and human immunodeficiency virus (HIV), mediate this process through trans-acting proteins (Rex and Rev, respectively) that bind to their cognate RNA targets (RxRE and RRE, respectively). The simple retroviruses do not encode such trans-acting proteins but rather use cis-acting sequences that presumably interact directly with cellular nuclear export proteins. One example is the CTE of

type D retroviruses, which is able to functionally replace Rev or RRE in subgenomic constructs and infectious HIV clones (1, 2). Here we report the identification and characterization of a candidate for the cellular cofactor of CTE.

Wild-type and a nonfunctional mutant CTE (Δ CTE) were biotinylated and used in RNA selection experiments (3, 4). A 140-kD protein was reproducibly selected by wild-type but not by mutant CTE (Fig. 1A, lanes 1 and 2). Use of a panel of CTE deletion mutants revealed a complete correlation of CTE function [as determined in a chloramphenicol acetyltransferase (CAT) reporter assay (4)] and the ability to select the 140-kD protein (Table 1). We separated the 140-kD protein from other cellular proteins by SDS-polyacrylamide gel electrophoresis (SDS-PAGE) and excised it from a polyvinylidene difluoride (PVDF) membrane after blotting. We subjected tryptic peptides to microsequencing as described (5). Three independently sequenced internal peptides matched with three different parts of one protein in a BLAST homology search: human adenosine triphosphate (ATP)-dependent RNA helicase A, a DEAD-box helicase that belongs to the

H. Tang, Department of Biology, University of California, San Diego, La Jolla, CA 92093, USA.

G. Gaietta and M. H. Ellisman, Department of Neurosciences, and San Diego Microscopy Imaging Resource, University of California, San Diego, La Jolla, CA 92093, USA.

W. H. Fischer, Clayton Foundation Laboratories for Peptide Biology, Salk Institute, La Jolla, CA 92097, USA.

F. Wong-Staal, Department of Medicine and Biology, University of California, San Diego, La Jolla, CA 92093-0665, USA.

*To whom correspondence should be addressed.

DEAH-box subfamily (6). We confirmed the identity of the 140-kD protein by immunoblotting with specific antibodies against human helicase A (Fig. 1A, lane 3). Direct interaction between CTE and helicase A was further shown by gel-shift experiments with purified protein. Complexes were formed between helicase A protein and CTE in the sense but not in the anti-sense orientation (Fig. 1B, lanes 1 to 4). There were two apparent complexes, suggesting that the protein might have oligo-

merized. Helicase A associates with and translocates along single-stranded tails of double-stranded RNA templates in vitro in the presence of ATP (7). We carried out RNA-protein interaction assays under the conditions used by Lee and Hurwitz (7). CTE remained bound to helicase A in the presence of ATP, suggesting that this interaction is not associated with the helicase activity of the protein (Fig. 1B, lanes 5 to 7).

The exact mechanism of CTE-mediated

nuclear export of unspliced mRNA is not clear, but because it can substitute for Rev or RRE function, the two pathways are likely to use a similar underlying mechanism. Rev shuttles between the nucleus and cytoplasm and contains a nuclear export signal in its activation domain (8, 9). Rev also appears in the cytoplasm with the overexpression of RRE-containing viral RNA (10). However, helicase A has not been observed previously to be a shuttling protein. We confirmed that the normal localization of helicase A is predominantly nuclear (Fig. 2A, a). In cells transiently transfected with pDM138CTE, a reporter construct in which CTE promotes CAT gene expression by exporting unspliced RNA containing the CAT sequences in an intron, the distribution of helicase A changed markedly, allowing detection of the protein at all stages of nuclear-cytoplasmic trafficking (Fig. 2A, b to e). In contrast, cells transfected with pDM128, which contains RRE instead of CTE in the intron (Fig. 2A, f); pDM138, which lacks CTE; and pDM138 Δ CTE, which contains a nonfunctional CTE, all retained helicase A predominantly in the nuclei (11). The cytoplasmic enrichment of helicase A in the presence of CTE is not likely due to a block of nuclear import of newly synthesized protein because treatment with the translation inhibitor cyclohexamide had no effect on cytoplasmic accumulation. Several other constructs that express CTE in different contexts (Fig. 2B) also induced cytoplasmic accumulation of helicase A (12), suggesting that CTE acts as a constitutive, position-independent signal that triggers nuclear export of helicase A.

Because not all the cells were transfected in the transient assay system used, we investigated whether cytoplasmic distribution of helicase A occurs in the same cells expressing CTE. Double labeling of the RNA and protein in CTE-transfected cells was carried out by in situ hybridization and immunostaining, and their subcellular lo-

Table 1. Specificity of interaction between CTE and helicase A. SRV, simian retrovirus; MPMV, Mason-Pfizer monkey virus.

CTE	CTE fragment	Ability to promote unspliced RNA export*	Interaction with helicase A†
SRV CTE	SRV(7620–7859)	+	+
MPMV CTE	MPMV(8005–8240)	+	+
Δ CTE	MPMV CTE(8128–8130) (AAA/TTT)	–	–
M19	MPMV(8005–8190)	+	+
M14	MPMV(8005–8140)	–	–
M21	MPMV(8031–8240)	–	–
CTE antisense	MPMV(8240–8005)	–	–

*Functional data were from a previous study; CTE function was assayed in the pDM138 system (4).

†Assayed by RNA-selection experiments.

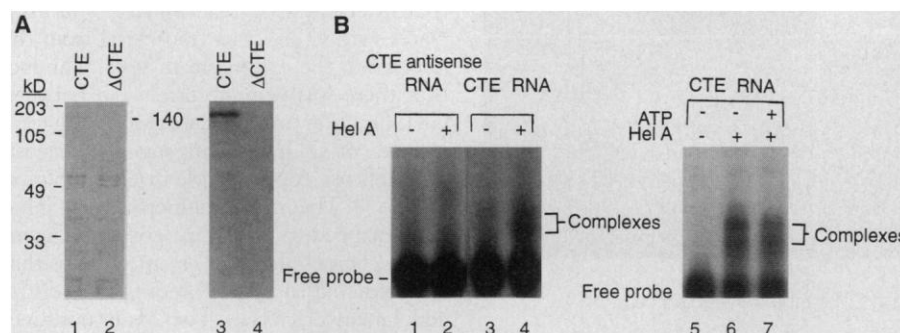
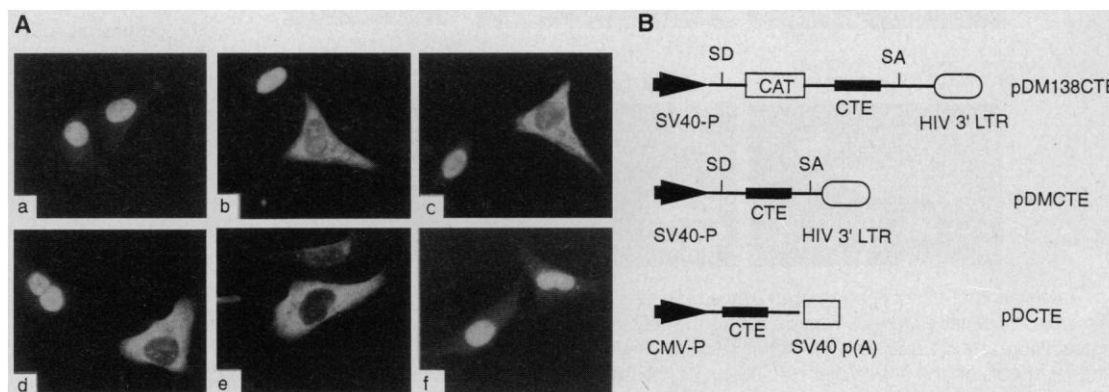


Fig. 1. In vitro interaction between CTE and human helicase A (23). **(A)** A 140-kD nuclear protein was specifically selected by wild-type (lane 1) but not mutant (lane 2) CTE. The protein was specifically recognized by a polyclonal antibody to human ATP-dependent RNA helicase A (lane 3). **(B)** Gel-shift assay of CTE with purified helicase A protein. Helicase A formed complexes with CTE but not with CTE antisense probe (lanes 1 to 4). Hydrolysis of ATP did not result in dissociation of the protein (lanes 5 to 7). The ATP chase experiments were done as described by Lee and Hurwitz (7).

Fig. 2. Helicase A shuttles between the cytoplasm and the nucleus in the presence of CTE-containing RNA (24). **(A)** (a) Helicase A concentrated in the nucleus in normal cells. (b to e) In cells transfected with pDM138CTE, helicase A was detected at all stages of nuclear-cytoplasmic trafficking. (f) Transfection of pDM128 did not change the normal nuclear distribution of the protein. **(B)** Three constructs were used in this study that expressed CTE in different contexts. pDMCTE is the same as pDM138CTE except that the CAT gene is deleted, leaving CTE alone in the intron; pDCTE is a construct in which the DNA fragment for CTE was cloned into pCDNA3; and CTE is now expressed as exon RNA.



calization was visualized by confocal microscopy. All cells that were negative for CTE staining also had no significant staining of helicase A in the cytoplasm, suggesting that the observed cytoplasmic accumulation of helicase A was a direct result of CTE overexpression. On the other hand, in cells expressing high levels of CTE in the cytoplasm, helicase A had relocated into the cytoplasm and associated with CTE (Fig. 3). The *in vivo* colocalization of CTE and helicase A was observed at various times after transfection and with different detection modules used to visualize RNA and protein in the cells (13). There were, however, some cells that expressed CTE in the cytoplasm while helicase A was still enriched in the nuclei, suggesting a dynamic process of RNA and protein shuttling in the transfected cells.

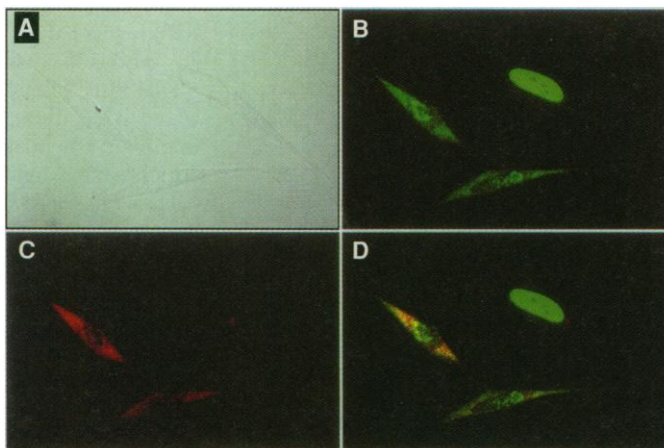
Rev and heterogeneous ribonucleoprotein (hnRNP) A1 are two well-characterized RNA-binding proteins involved in RNA transport. They accumulate in the cytoplasm with inhibition of transcription (8, 14), suggesting that ongoing transcription is required for the rapid shuttling of these proteins back to the nuclei. To determine whether helicase A has intrinsic shuttling capability, we treated HeLa cells for 3 hours with various transcriptional inhibitors and stained the cells with antibodies to helicase A. Redistribution of helicase A to the cytoplasm was observed when the cells were treated with actinomycin D (5 $\mu\text{g/ml}$) and kept at 37°C (Fig. 4A, lower right). Nuclear localization of the protein was retained in untreated cells or in treated cells kept at 4°C after addition of actinomycin D (Fig. 4A, upper), suggesting that nuclear

export of the protein is energy-dependent. Treatment with actinomycin D did not make the nuclei generally leaky because the distribution of another nuclear protein, splicing factor SC35, was not altered (Fig. 4B). Again, treatment of the cells with cyclohexamide (50 $\mu\text{g/ml}$) had no effect on the cytoplasmic distribution of helicase A in the presence of actinomycin D, suggesting that the cytoplasmic staining was a result of export of preexisting protein. 5,6-Dichlorobenzimidazole riboside (DRB; 100 μM), which inhibited RNA polymerase II (Pol II) and promoted cytoplasmic accumulation of Rev and hnRNP A1 in the cytoplasm (8, 13, 15), did not alter nuclear localization of helicase A. In addition, actinomycin D (0.04 $\mu\text{g/ml}$) alone, which is sufficient to inhibit RNA Pol I transcription (16), or in combination with 100 μM DRB, also had no effect (17) (Fig. 4A, lower left). Thus, these data in combination with the observation that actinomycin D (5 $\mu\text{g/ml}$) inhibits transcription by all three RNA polymerases suggest that inhibition of Pol III transcription is necessary for cytoplasmic accumulation of helicase A.

In summary, we have identified RNA helicase A as an inherent shuttling protein that interacts with CTE *in vitro* and associates with CTE in its trafficking from the nucleus to the cytoplasm *in vivo*. The fact that there was perfect correlation between CTE function and helicase A binding for a number of CTE mutants strongly suggests that helicase A plays a role in CTE function (Table 1). The minimal functional CTE has been mapped to a 173-nucleotide fragment and is composed of two essential loops that are predicted to be the binding sites of the cellular cofactors (18). Two of our nonfunctional mutants (M21 and M14) contain deletions that destroy formation of loop A without affecting loop B (Table 1), whereas ΔCTE contains mutations that are predicted by computer analysis to unravel the stem structure between the loops and thus affect formation of both loops. The failure of helicase A to bind to all three mutants suggests that loop A of CTE is required for the interaction and, as in the case for CTE function, loop B alone is not sufficient for binding to helicase A even though loops A and B have identical sequences (19). We have previously identified two additional nuclear proteins that bind to wild-type CTE but not to ΔCTE (4). Therefore, other proteins may be involved in CTE-mediated gene expression.

Several DEAH-box RNA helicases participate in mRNA transport. A 144-kD human helicase-like protein, human RNA helicase 1, facilitated export of cellular mRNA by releasing the RNA from the spliceosome after splicing was completed

Fig. 3. Helicase A colocalizes with CTE *in vivo*. HeLa cells were fixed 20 hours after transfection. CTE and helicase A were detected by combining *in situ* hybridization (CTE) and immunostaining (helicase A) techniques. (A) Transmitted light image. (B) Immunodetection of helicase A. (C) Detection of CTE-containing RNA by *in situ* hybridization with digoxigenin-labeled antisense RNA probe. Both positively transfected and untransfected cells are shown.



(D) Double labeling reveals colocalization of helicase A and CTE in the transfected cells.

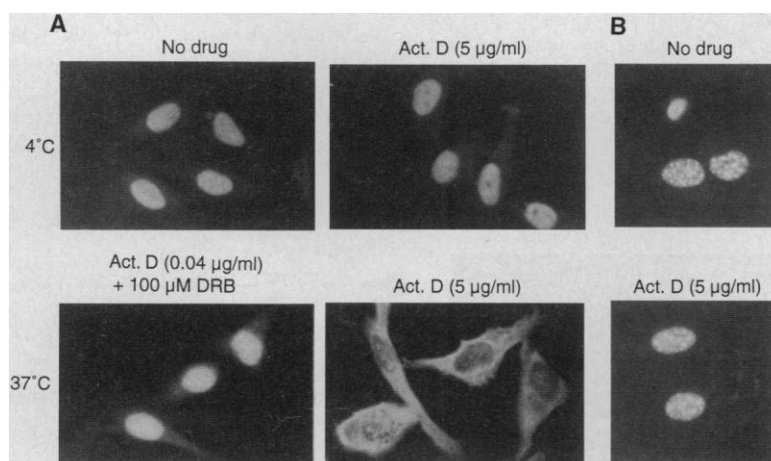


Fig. 4. Inhibition of transcription accumulates helicase A in the cytoplasm. Cyclohexamide (50 $\mu\text{g/ml}$) was added to all cell cultures 3.5 hours before the cells were fixed. Helicase A was detected by indirect immunofluorescence labeling (20). (A) Inhibitors of RNA synthesis by various RNA polymerases had different effects on the subcellular distribution of helicase A. Inhibition of Pol I and Pol II transcription [actinomycin D (0.04 $\mu\text{g/ml}$) and 100 μM DRB] did not cause significant change of nuclear localization of the protein, whereas actinomycin D (5 $\mu\text{g/ml}$) accumulated helicase A in the cytoplasm at 37°C. (B) Actinomycin D (5 $\mu\text{g/ml}$) treatment did not alter nuclear localization of splicing factor SC35.

(20). A yeast gene capable of encoding a 120-kD putative RNA helicase protein rescued the mutant phenotype of a conditional yeast mutant defective in export of polyadenylated RNA (21). Given the RNA-binding and shuttling ability of helicase A, it is conceivable that it participates in certain cellular RNA export pathways. Simian retroviruses have likely tapped into this pathway and use helicase A as a cofactor in nuclear export of CTE-containing RNA by means of a specific RNA-protein interaction. It will be interesting to determine whether helicase A also plays a role in the replication cycle of other retroviruses, including complex retroviruses such as HIV.

REFERENCES AND NOTES

1. M. Bray *et al.*, *Proc. Natl. Acad. Sci. U.S.A.* **91**, 1256 (1994).
2. A. S. Zolotukhin, A. Valentin, G. N. Pavlakis, B. K. Felber, *J. Virol.* **68**, 7944 (1994).
3. J. M. Yeakley, J. P. Morfin, M. G. Rosenfeld, X. D. Fu, *Proc. Natl. Acad. Sci. U.S.A.* **15**, 7582 (1996).
4. H. Tang, Y. Xu, F. Wong-Staal, *Virology* **228**, 333 (1997).
5. Y. Xu, W. H. Fischer, T. R. Reddy, F. Wong-Staal, *J. Biomed. Sci.* **3**, 82 (1996).
6. Sequences of three microsequenced peptides are as follows: peptide 1, AENN(C)EVGA(C)GYGGVXG (matching amino acids 121 to 136 of helicase A); peptide 2, YTVQVDPDHNH (matching amino acids 200 to 209 of helicase A); peptide 3, LAQFEPSSQRF (matching amino acids 315 to 323 of helicase A) (22); C. Lee and J. Hurwitz, *J. Biol. Chem.* **268**, 16822 (1993).
7. C. Lee and J. Hurwitz, *J. Biol. Chem.* **267**, 4398 (1992).
8. B. E. Meyer and M. H. Malim, *Genes Dev.* **8**, 1538 (1994).
9. U. Fischer, J. Huber, W. C. Boelens, I. W. Mattaj, R. Luhrmann, *Cell* **82**, 475 (1995).
10. L. Luznik, *et al.*, *AIDS Res. Hum. Retroviruses* **11**, 795 (1993).
11. H. Tang and F. Wong-Staal, unpublished data.
12. H. Tang, G. M. Gaietta, W. H. Fischer, M. H. Ellisman, F. Wong-Staal, data not shown.
13. The sense and antisense RNA probes were prepared by *in vitro* transcription, with 2'-deoxyuridine-5'-triphosphate coupled to digoxigenin (digoxigenin-11-dUTP) (Boehringer Mannheim) as a label. HeLa cells were attached to glass cover slips (Fisher) coated with poly-D-lysine (Sigma). Sixteen, 20, and 26 hours after the addition of DNA-calcium precipitate, cells were washed in phosphate-buffered saline (PBS) until no precipitate was visible and then fixed with 4% paraformaldehyde for 30 min. The following steps were performed to facilitate accessibility of CTE and to reduce nonspecific binding of the RNA probe: 2 min in 0.5% Triton X-100 (in PBS), 5 min in 0.5 N HCl, 10 min in acetylation buffer (583 μ l of triethanolamine and 125 μ l of acetic anhydride in 50 ml of diethyl pyrocarbonate-treated water). Each step was followed by two brief washes in PBS, and then 30 μ l of prehybridization solution [containing 50% formamide, 5 \times standard saline citrate (SSC), 5 \times Denhardt's reagent, single-stranded DNA (50 μ g/ml), tRNA (25 μ g/ml)] lacking the probe was applied to each sample. Samples were prehybridized at 42°C for 1 hour in a humid chamber. At the end of the prehybridization step, samples were rinsed in 5 \times SSC and prepared for the hybridization step: 30 μ l of prehybridization solution, containing a 1:100 dilution of the digoxigenin-labeled RNA probes (previously denatured at 65°C for 10 min) was applied to each cover slip, covered with a glass coverslip, and sealed with rubber cement. Hybridization was carried out overnight at 42°C in a humid chamber. The posthybridization washes were performed in SSC wash buffer at high stringency (2 \times to 0.1 \times). Samples

were treated with ribonuclease to remove RNA probes that did not hybridize to the target RNA. Detection of the hybridized RNA probes was performed with an antibody to digoxigenin F(ab) coupled to alkaline phosphatase (Boehringer Mannheim) followed by a colorimetric reaction with nitroblue tetrazolium and 5-bromo-4-chloro-3-indolyl phosphate, or by hybridization with a biotinylated secondary antibody and detection with streptavidin Cy5 conjugate. The protein was detected with a rabbit polyclonal antibody to human helicase A. The polyclonal antibody was then immunodetected with a donkey antibody to rabbit immunoglobulin G coupled to Cy5 (detection of RNA probe with alkaline phosphatase) or to fluorescein isothiocyanate (FITC) (RNA indirectly labeled with Cy5). The samples were viewed with a Bio-Rad MRC 1024 laser-scanning confocal system coupled to a Zeiss Axiovert 35M microscope with a planapochromatic objective (\times 40, 1.3 numerical aperture, oil immersion).

14. S. Piñol-Roma and G. Dreyfuss, *Nature* **355**, 730 (1992).
15. F. B. Sehgal, J. E. Darnell, I. Tamm, *Cell* **9**, 473 (1976).
16. R. P. Perry and D. E. Kelly, *J. Cell. Physiol.* **76**, 127 (1970).
17. H. Tang and F. Wong-Staal, unpublished data.
18. C. Taberner, A. S. Zolotukhin, A. Valentin, G. N. Pavlakis, B. K. Felber, *J. Virol.* **70**, 5998 (1996).
19. R. K. Ernst, M. Bray, D. Rekosh, M. Hammarskjöld, *Mol. Cell. Biol.* **17**, 135 (1997).
20. M. Ohno and Y. Shimura, *Genes Dev.* **10**, 997 (1996).
21. S. Liang, M. Hitomi, Y. Hu, Y. Liu, A. M. Tartakoff, *Mol. Cell. Biol.* **16**, 5139 (1996).
22. Abbreviations for the amino acid residues are: A, Ala; C, Cys; D, Asp; E, Glu; F, Phe; G, Gly; H, His; I, Ile; K, Lys; L, Leu; M, Met; N, Asn; P, Pro; Q, Gln; R, Arg; S, Ser; T, Thr; V, Val; W, Trp; and Y, Tyr.
23. Large amounts of biotinylated RNA were made with the Megashortscript *in vitro* transcription kit (Ambion) in the presence of biotin-21-UTP (Clontech). Nuclear extract (200 μ l) was incubated with about 100 μ g of biotinylated CTE wild-type or mutant RNA at 4°C overnight before being subjected to affinity purification with streptavidin-conjugated agarose beads (BRL). Proteins that were trapped in beads were eluted by

eating in SDS-PAGE buffer at 65°C for 5 min and then run on a 6% polyacrylamide gel. Proteins were either visualized by Coomassie blue staining, tranship; &5qferred onto a PVDF membrane and stained with 0.1% amido black 10B, or detected by antibodies. For protein internal sequence determination, the protein band was excised from the PVDF membrane and subjected to trypsin digestion, peptides were purified by high-performance liquid chromatography, and three well-separated fractions were selected for microsequencing. RNA used in gel-shift assays was labeled with [³²P]UTP and purified from polyacrylamide gel. Purified human helicase A (100 to 200 ng) was then incubated with RNA probe (1 \times 10⁵ cpm) for 15 min at room temperature. The reaction mixture was then mixed with RNA loading buffer (10% glycerol, 0.01% bromophenol blue, 0.01% xylene cyanol) and run on a 4% polyacrylamide gel (acrylamide:bisacrylamide = 60:1). The gel was subsequently dried and subjected to autoradiography.

24. HeLa cells were grown in slide chambers. Transfections were done by conventional calcium phosphate precipitation and cells were fixed for immunostaining 26 to 28 hours after transfection. Cells were fixed in methanol and acetone (1:1) for 2 min, washed extensively with PBS, and blocked with 3% bovine serum albumin in PBS for 10 min before the first antibodies were applied. The polyclonal antibody against helicase A was provided by Lee and Hurwitz (6). FITC-coupled goat antibody to rabbit immunoglobulin G was used as a second antibody to detect helicase A. Cells grown on coated glass cover slips, fixed with 4% paraformaldehyde, and permeabilized by 0.5% Triton X-100 gave essentially the same results for protein staining.
25. We are indebted to C. Lee and J. Hurwitz for purified helicase A protein and a polyclonal antibody against human helicase A. R. Moy helped with the constructions of pDMCTE and pDCTE. M. Park performed the protein sequence analysis. Supported in part by grants NIH RR 04050 and NS 14718 (M.H.E.) and by the University of California, San Diego, Center for AIDS Research (F.W-S).

16 January 1997; accepted 4 April 1997

Induction of Leaf Primordia by the Cell Wall Protein Expansin

Andrew J. Fleming,* Simon McQueen-Mason, Therese Mandel, Cris Kuhlemeier†

Expansins are extracellular proteins that increase plant cell wall extensibility *in vitro*. Beads loaded with purified expansin induced bulging on the leaf-generating organ, the apical meristem, of tomato plants. Some of these bulges underwent morphogenesis to produce leaflike structures, resulting in a reversal of the direction of phyllotaxis. Thus, expansin can induce tissue expansion *in vivo*, and localized control of tissue expansion may be sufficient to induce leaf formation. These results suggest a role for biophysical forces in the regulation of plant development.

Leaves form by reiterative organogenesis from a specialized organ, the shoot apical meristem (1). Although spatial domains of transcription factor activity can dictate where and when a leaf is initiated, the mechanism by which this information is transduced into morphogenesis is unknown (2). One model predicts that the regulation of epidermal cell wall extensibility controls tissue expansion and thus the initial steps of primordium formation

(3). Recently, a family of cell wall proteins, expansins, that modulate cell wall extension *in vitro* has been characterized, although the ability of these proteins to induce cell expansion *in vivo* was not demonstrated (4). We now show that the localized application of expansin to the apical meristem induces expansion in living tissue and that the resultant bulging is sufficient to induce primordium formation.

In the tomato plant, leaves are initiated